# Mechanical force effect on the two-state equilibrium of the hyaluronan-binding domain of CD44 in cell rolling

Takashi Suzuki, Miho Suzuki, Shinji Ogino, Ryo Umemoto, Noritaka Nishida, and Ichio Shimada[1]

Division of Physical Chemistry, Graduate School of Pharmaceutical Sciences, University of Tokyo, Tokyo 113-0033, Japan

CD44 is the receptor for hyaluronan (HA) and mediates cell rolling under fluid shear stress. The HA-binding domain (HABD) of CD44 interconverts between a low-affinity, ordered (O) state and a high-affinity, partially disordered (PD) state, by the conformational change of the C-terminal region, which is connected to the plasma membrane. To examine the role of tensile force on CD44-mediated rolling, we used a cell-free rolling system, in which recombinant HABDs were attached to beads through a C-terminal or N-terminal tag. We found that the rolling behavior was stabilized only at high shear stress, when the HABD was attached through the C-terminal tag. In contrast, no difference was observed for the beads coated with HABD mutants that constitutively adopt either the O state or the PD state. Steered molecular dynamics simulations suggested that the force from the C terminus disrupts the interaction between the C-terminal region and the core of the domain, thus providing structural insights into how the mechanical force triggers the allosteric O-to-PD transition. Based on these results, we propose that the force applied from the C terminus enhances the HABD–HA interactions by inducing the conformational change to the high-affinity PD transition more rapidly, thereby enabling CD44 to mediate lymphocyte trafficking and hematopoietic progenitor cell homing under high-shear conditions.

cell adhesion | allosteric regulation | mechanical force | CD44 | hyaluronan

Leukocyte extravasation from blood to sites of infection and inflammation or to specific organs is achieved by a sequential adhesion cascade: (*i*) rolling, (*ii*) chemokine-induced activation, (*iii*) firm adhesion, and (*iv*) transcellular migration. Rolling is mediated by specialized cell surface adhesion molecules, such as selectins, CD44, and specific types of integrins (1, 2).

Under conditions of hydrodynamic flow, receptor–ligand bonds are subjected to tensile mechanical force, which disrupts the receptor–ligand bond (Fig. 1*A*). In general, the lifetime of the receptor–ligand bond exponentially decreases with an increase of the mechanical force (3). However, there is growing evidence demonstrating that the lifetimes of some receptor–ligand bonds increase when moderate levels of force are applied (4–9). However, the underlying mechanism of this phenomenon is still elusive and in some cases controversial. For example, integrin and bacterial adhesin FimH-mediated adhesion have been explained by an "allosteric model," in which mechanical force induces allosteric changes of the receptor, resulting in the stabilization of the high-affinity state (10, 11). Although selectin-mediated adhesion has been explained by the allosteric model (12), a different "sliding-rebinding model" was also reported (13). This model proposes that force tilts the binding interface to make it parallel to the direction of force, allowing the selectin ligand to slide on the selectin and to form new contacts. The sliding-rebinding model has also been used to explain the force-induced activation of von Willebrand factor-mediated adhesion and actin depolymerization (6, 8).

CD44 is a transmembrane receptor for hyaluronan (HA) (14). CD44–HA interactions are involved in various physiological and pathological processes mediated over a wide range of hydrodynamic forces, including T-lymphocyte trafficking on the endothelium (15, 16), hematopoietic progenitor cell homing into bone marrow niches (17), and the progression of atherosclerosis (18).

The HA-binding domain (HABD) of CD44 adopts two distinctive conformations representing the low- and high-affinity states for HA (19–21). HABD is composed of a conserved Link module and the N- and C-terminal extension segment (22). In the ordered (O) state, the C-terminal segment is well folded (Fig. 1*B*) (19), whereas it becomes disordered in the partially disordered (PD) state upon ligand binding (Fig. 1*C*) (20). In addition, solution NMR analyses demonstrated that HABD exists in an equilibrium between the O and PD states in both the HA-unbound and HA-bound states, with a transition rate of ~500 ms, and that HA binding induces an equilibrium shift toward the PD state (21) (Fig. 1*D*). The Y161A mutant, which constitutively adopts the PD state, exhibits a higher affinity than wild-type HABD, indicating that the O and PD states represent the low- and high-affinity states for HA, respectively (21) (Fig. 1*E*). Cells expressing the Y161A mutant exhibited firm adhesion and impaired rolling on an HA substrate, suggesting that the two-state conformations are essential for the CD44-mediated rolling under flow conditions (21).

Despite the importance of the mechanical force in rolling, the means by which it affects the CD44-mediated rolling remain poorly characterized. Recently, it was reported that the rolling of CD44-expressing cells is enhanced at the higher shear stress (23), raising the possibility that CD44 possesses some mechanochemical specializations to resist higher tensile force. Considering the fact that the C terminus of CD44 HABD is connected to the plasma membrane, the force applied from the C terminus of HABD would induce the allosteric transition from the O to the PD state, thereby providing the resistance to the applied force. On the other hand, our previous NMR studies demonstrated that more than 90% of HABD adopts the PD state in the HA-bound state (21), indicating that the free energy of the PD state can be lowered upon HA binding, regardless of the presence or

## Significance

Rolling is a first step for cells to transmigrate across the endothelium and is mediated by specialized adhesion receptors. Although it has been demonstrated that the mechanical force positively regulates rolling mediated by selectins and integrins, it remains elusive how force affects the rolling mediated by a hyaluronan receptor, CD44. Here, we demonstrate that the force applied from the C terminus of the hyaluronan-binding domain of CD44 stabilized the CD44-mediated rolling. We also found that the effect of force is to shorten the transition time from the low- to the high-affinity state. The mechanism described here provides the structural basis for the CD44-mediated rolling, which is important for lymphocyte trafficking and the stem cell homing.
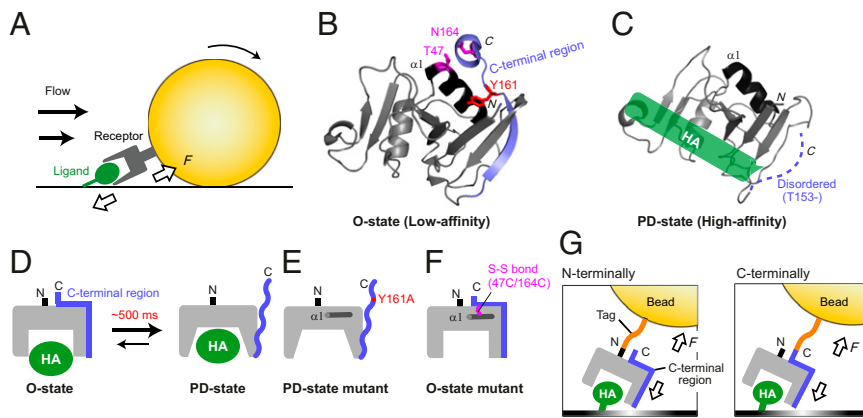
**Fig. 1.** The effect of the tensile force on the two-state conformations of CD44 HABD. (*A*) Illustration of the tensile force applied between the receptor on the cells and the immobilized ligand under the fluid shear force. (*B*) The crystal structure of CD44 HABD in the HA-unbound O state (PDB code: 1UUH). The C-terminal region and the α1 helix are colored blue and black, respectively. The residues that were mutated to lock in the O state (T47, N164) and to stabilize the PD state (Y161) are indicated by magenta and red sticks, respectively. (*C*) The NMR structure of HABD in the HA-bound PD state (PDB code: 2I83). The HA-binding site is indicated by a green box. (*D*) A schematic illustration of the conformational transition between O state and PD state, which occurs on the timescale of 500 ms in solution. (*E* and *F*) Design of the HABD mutants that adopt only the PD state (*E*) and the O state (*F*). (*G*) Schematic illustration of the cell-free rolling experiment to examine the effect of the tensile force, using beads with either N- or C-terminally attached HABD.

absence of the tensile force. Therefore, it is worthwhile to investigate whether the CD44–HA interaction is strengthened by the tensile force.

To assess the effect of the tensile force on the CD44-mediated rolling, we established a cell-free rolling system using cell-sized beads, which are coated with recombinant HABDs. The effect of the tensile force can be investigated by comparing the rolling activity of the beads coated with the ligand-binding domain via the N-terminal or the C-terminal tag (Fig. 1*G*) (10). We compared the rolling behavior of the beads with N- or C-terminally attached HABD and found that the rolling behavior was stabilized only at higher shear stress, when HABD was attached to the beads via the C-terminal tag. Steered molecular dynamics (SMD) simulations suggested that the force from the C terminus induces the dissociation of the "mechanosensitive latch" in the C-terminal region, which triggers the conversion from the O to the PD state. Based on these results, we propose that the tensile force from the C terminus stabilizes the CD44–HA bond by inducing a rapid transition from the O to the PD state, thereby sustaining the CD44-mediated cell rolling under higher shear stress conditions.

## Results

**Rolling Analyses in a Cell-Free System.** To immobilize HABD on beads by biotin–avidin chemistry, the HABD construct containing the AviTag at the C terminus was expressed and subjected to in vitro biotinylation by biotin ligase (BirA). We confirmed that the attachment of the AviTag did not affect the conformation and the HA-binding affinity of HABD, by NMR and surface plasmon resonance (SPR) analyses, respectively (Fig. S1 and Table S1). The C-terminally biotinylated wild-type (WT) HABD was then immobilized to the avidin-coated beads with a 10 μm diameter, which is equivalent to the size of mammalian lymphocytes. The rolling behavior of the HABD-immobilized beads was investigated by perfusing them in a parallel plate laminar flow chamber, in which the bottom surface was coated with the HA ligand (Table S2). The HABD-coated beads exhibited initial tethering and subsequent rolling behaviors on the HA surface. The rolling velocity was similar to that observed in previous rolling experiments, using mammalian cells expressing intact CD44 (21). We confirmed that the adhesion behaviors were mediated by the specific interaction between HABD and HA, based on following results: (*i*) The HABD-coated beads did not

adhere to the plate without the HA immobilization, and (*ii*) the beads without the HABD immobilization did not adhere to the HA-coated plate. Therefore, we concluded that the CD44-mediated rolling was successfully reconstituted by the cell-free rolling system.

We compared the rolling behavior of beads coated with WT HABD to that of beads coated with the PD-state mutant via the C-terminal tag. First, we prepared beads, bearing nearly equal amounts of either WT HABD or the PD-state mutant (Fig. S2). The rolling behavior was measured by the detachment assay, as follows. The beads were allowed to accumulate on the HA-coated surface for 5 min at a low shear stress of 0.3 dyn/cm² and then subjected to increasing shear stress up to 2.0 dyn/cm². The rolling behavior of the beads was quantified by two parameters: (*i*) the percentage of beads remaining bound and (*ii*) the average rolling velocity at each shear stress. In the detachment assay, both the WT HABD-coated beads and the PD-state mutant-coated beads showed stable adhesion even at higher shear stress, although the PD-state mutant was somewhat more shear resistant than WT (Fig. 2*A*). However, the averaged rolling velocities revealed that the PD-state mutant-coated beads mainly exhibited firm adhesion, whereas the WT HABD-coated beads exhibited rolling (Fig. 2*B*). These results are consistent with those of previous rolling experiments, using human cancer cells stably transfected with CD44 (21).

**Transition from the O to the PD State Is Necessary for Shear Resistance.** To further demonstrate the significance of the two conformational states of HABD in the cell rolling, we designed a mutant in which the conformation was locked in the O state. To stabilize the O-state conformation, T47 in the α1 helix in the Link module and N164 in the C-terminal extension region, which are close to each other in the crystal structure of HABD in the O state, were substituted with Cys to form an intradomain disulfide bond (Fig. 1 *B* and *F*). We confirmed that the T47C/N164C mutant forms an additional disulfide bond. The NMR spectrum of the mutant exhibited only the signals corresponding to the O state, indicating that the conformation of the T47C/N164C mutant was locked in the O state (Fig. S3). By SPR analyses, the dissociation constant ($K_D$) of the T47C/N164C mutant was estimated to be 53 μM, which was twofold lower than that of WT. Therefore, these results supported that the T47C/N164C mutant exclusively adopts the low-affinity conformation of the O state. Hereafter, we refer to the T47C/N164C mutant as the O-state mutant.
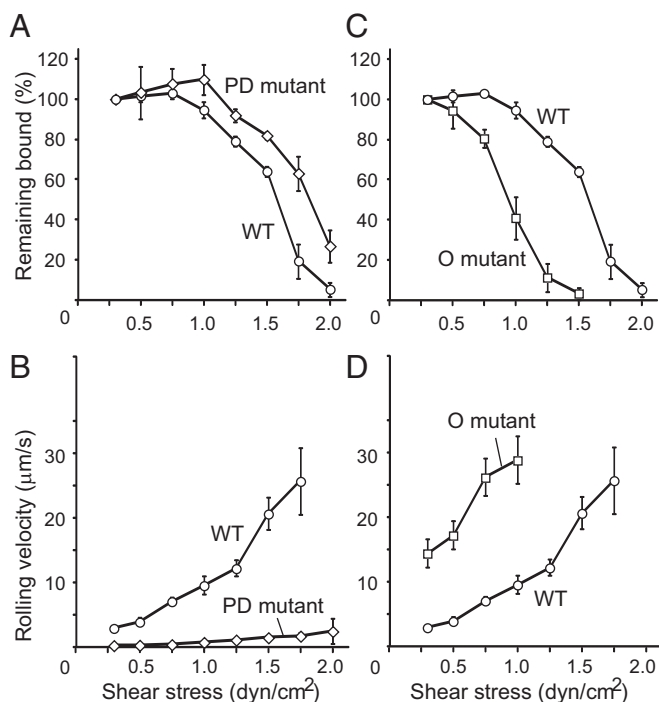
**Fig. 2.** Rolling activities of beads coated with wild-type HABD, the PD-state mutant, and the O-state mutant through the C-terminal anchoring. (*A–D*) Results of the detachment assays using beads coated with the PD-state mutant (*A* and *B*, open diamonds) and the O-state mutant (*C* and *D*, open squares), in comparison with those coated with the wild type (open circles). The percentages of beads remaining bound (*A* and *C*) and the mean velocities (*B* and *D*) were plotted at each shear stress.

We prepared beads coated with the O-state mutant via the C-terminal tag and performed the detachment assay. Overall, the beads coated with the O-state mutant mainly exhibited rolling with a faster velocity than the beads with WT HABD (Fig. 2*D*). Notably, as the shear stress increased, fewer beads were able to continue rolling and almost all beads were detached at 1.5 dyn/cm$^2$, indicating that the shear resistance of the beads coated with the O-state mutant was weaker than that of the beads coated with WT HABD and the PD-state mutant (Fig. 2*C*). The completely different rolling behaviors between the O- and the PD-state mutants further support the existence of two legitimate states in HABD. In addition, the reduced shear resistance of the O-state mutant clearly indicates that the transition from the O to the PD state upon ligand binding is necessary to increase the resistance to the detachment at high shear stress. Therefore, we concluded that the conformational transition from the O to the PD state is necessary for CD44 to mediate the cell rolling under a wide range of shear stresses.

**Only the Force Applied from the C Terminus Stabilizes the Rolling Under Higher Shear Forces.** Next, we compared the rolling activity of beads coated with WT HABD, through either the N-terminal or the C-terminal tag (Fig. 1*G*). Given that the tensile force from the C terminus could promote the transition from the O to the PD state, it is expected that the beads with the C-terminally attached HABD would be more resistant to the shear forces, compared with those with the N-terminally attached HABD. First, we confirmed that the affinity for HA was equivalent between the N- and C-terminally tagged WT HABDs in solution (Table S1). We also confirmed that almost equal amounts of HABD with the N-terminal and C-terminal tags were immobilized on the beads (Fig. 3*A*). In the detachment assay, the beads with the N- and C-terminally attached HABDs both

exhibited stable rolling at lower shear stresses below 0.75 dyn/cm$^2$ (Fig. 3 *B* and *C*). The average rolling velocity was also similar between the beads with N-terminally and C-terminally attached WT HABD below 0.5 dyn/cm$^2$ (Fig. 3*C*). On the other hand, the rolling velocity of the beads with the N-terminally attached WT HABD increased faster than that of the beads with the C-terminally attached WT HABD at shear stresses above 1.0 dyn/cm$^2$. The average rolling velocities of the beads with N- and C-terminally attached WT HABD at 1.25 dyn/cm$^2$, for example, were 23 ± 2 μm/s and 12 ± 1 μm/s, respectively (Fig. 3*C*). Furthermore, the beads with the N-terminally attached WT HABD detached rapidly at high shear force, and only 10% of those remained attached at 1.5 dyn/cm$^2$ (Fig. 3*B*). In contrast, more than 60% of the beads with the C-terminally attached WT HABD continued rolling at 1.5 dyn/cm$^2$ (Fig. 3*B*). These results indicate that the rolling mediated by the N-terminally attached WT HABD was sustained less under high shear stress conditions than that by the C-terminally attached WT HABD.

Next, we compared the rolling activity of the beads coated with the PD-state mutant through the N- or the C-terminal tag. Because no conformational change would be induced by the mechanical force in those mutants, it was expected that the rolling behavior would not be affected by the directionality of the force. Indeed, the percentage of the remaining bound beads was similar between the beads with the N-terminally and C-terminally attached PD-state mutant, along a wide range of shear stresses. The beads with the N-terminally and C-terminally attached PD state remained adhered below 1.5 dyn/cm$^2$ and suddenly detached at 1.75 dyn/cm$^2$ and 2.0 dyn/cm$^2$, respectively (Fig. 3*D*). The rolling velocity was also similar between the beads with the N- and C-terminally attached PD-state mutants (Fig. 3*E*), indicating that the PD-state mutant exhibited firm adhesion, regardless of the directionality of immobilization.

Finally, we also compared the rolling activities of the beads with the N-terminally and C-terminally attached O-state mutant. Similar to the PD-state mutant, no significant difference was found: Both exhibited weaker shear resistance and almost all of the beads detached by 1.5 dyn/cm$^2$ (Fig. 3*F*). The rolling velocity also increased rapidly, as the shear stress increased (Fig. 3*G*). All of these results support the hypothesis that the force applied from the C terminus of HABD facilitates the transition from the O to the PD state and thus stabilizes the CD44-mediated rolling under higher shear stress conditions.

**Conformational Transition Triggered by the Dissociation of the Mechanosensitive Latch.** We performed SMD simulations to explore how the force applied from the C terminus changes the conformation of CD44 HABD. As the initial structure for the SMD simulation, we used the crystal structure of mouse CD44 HABD in complex with an HA octamer that adopts the O-state conformation (24). Because the ligand binding induces the equilibrium shift from the O to the PD state (21), this structure would reflect the complex structure that is formed by the initial contact between HABD on the beads and the immobilized HA. During the simulation, the C terminus of HABD was pulled at a constant velocity. On the other hand, one HA atom located in the center of the octamer chain was held fixed, which resembles the physiological situations where the HA chains are stably immobilized on the surface of the endothelium. Throughout the simulation period of 4 ns (Fig. S4), the interaction between HABD and HA was sustained against the pulling force (Fig. 4*A*). For instance, the hydrogen bond between the carbonyl oxygen of Ile100 and the amide nitrogen of *N*-acetylglucosamine (NAG) was stably formed (Fig. 4*B*), suggesting that the interaction between HABD and HA is strong enough to resist the pulling force. Whereas the structure of HABD also remained mostly unchanged by the pulling force, a significant conformation change was observed for the C-terminal region of HABD
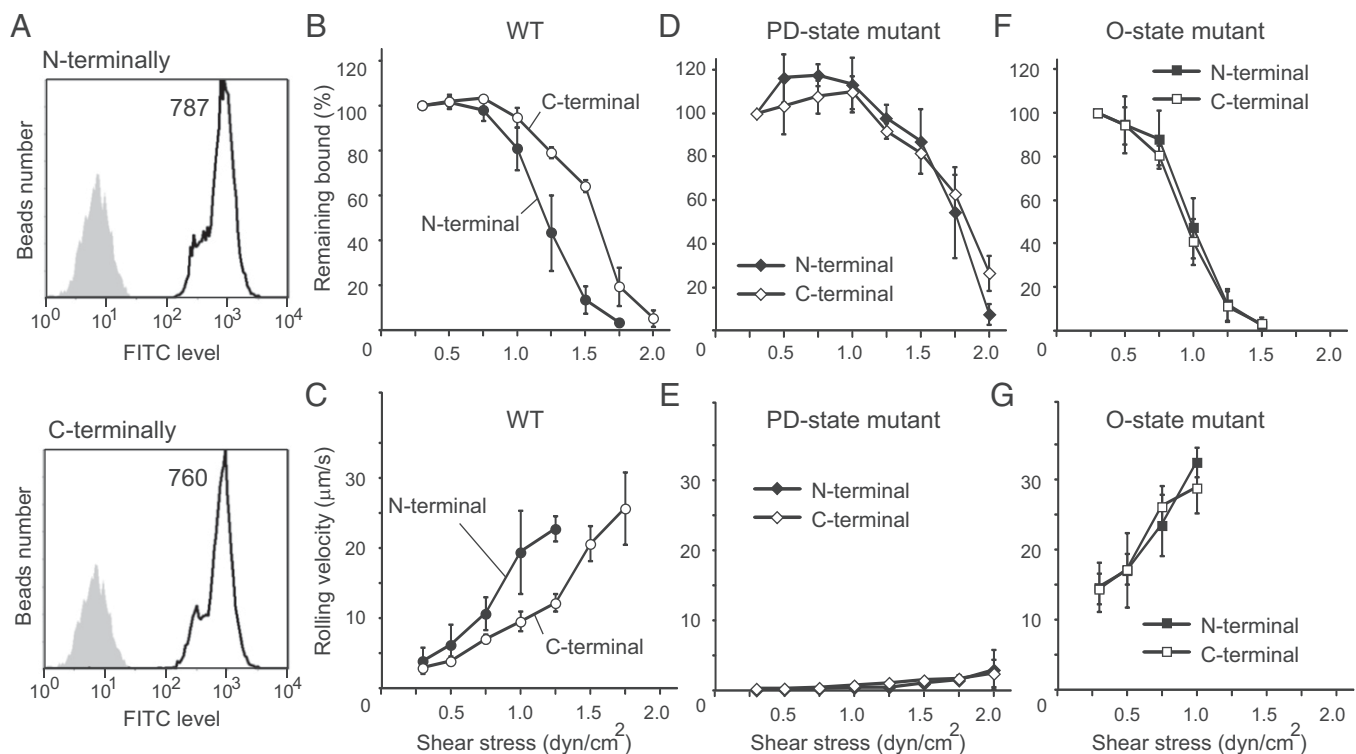
**Fig. 3.** Rolling activities of beads coated with the N- or C-terminally attached HABDs. (*A*) Estimation of the amounts of HABD immobilized on the beads, by flow cytometry analyses. The beads with the N- or C-terminally attached HABD (open profiles) and those without immobilization (shaded profiles) were compared. Mean fluorescence values are indicated in the plot. (*B–G*) The results of the detachment assays were compared between the beads with the N-terminally (solid symbols) and the C-terminally (open symbols) attached WT HABD (*B* and *C*), the PD-state mutant (*D* and *E*), and the O-state mutant (*F* and *G*). The percentages of beads remaining bound (*B*, *D*, and *F*) and the mean velocities (*C*, *E*, and *G*) were plotted at each shear stress.

(residues 166–178). This region, which was initially docked into the α1 helix, became detached in the course of the SMD simulation (Fig. 4*A*). The hydrogen bond between a hydroxyl group of Y166 (corresponding to Y161 in human CD44) and the hydroxyl group of E52 (corresponding to E48 in human CD44) was disrupted at ∼3 ns (Fig. 4*B*). This result is consistent with the fact that the substitution of Y161 with Ala destabilizes the O state, and the mutant HABD adopts only the PD state (21). The results of the SMD simulation suggest that the mechanical force facilitates rapid conformational rearrangements from the O to the PD state by releasing the mechanically weak interaction between the α1 helix and the C-terminal region, which we refer to as a mechanosensitive latch. Therefore, we propose that mechanical force induces the dissociation of the C-terminal mechanosensitive latch from the α1 helix and thus facilitates the allosteric transition to the PD state (Fig. 4*C*).

## Discussion

In the present study, we reconstituted CD44-mediated cell rolling by using beads bearing recombinant HABD, attached via a biotinylated tag. By using the cell-free system, the rolling experiments can be performed under well-controlled conditions (25), without heterogeneities derived from cellular features, such as cell sizes and shapes, CD44 expression level, other endogenous proteins, and posttranslational modifications. Therefore, the cell-free rolling system, using WT HABD and its mutants stabilized in the O or the PD state, allowed us to investigate the CD44-mediated rolling in a quantitative manner. It should be mentioned that the rolling behaviors are not identical between the cells expressing CD44 and the beads displaying the HABD. For instance, the stabilization of the rolling (e.g., increase of adhesion numbers or decrease of rolling velocities) at high shear

stress was observed only for the experiments using cells (21, 23). Those differences may be ascribed to the cellular features, such as the formation of microvilli, slings (26), and cell flattening, which also contribute to stable rolling (27).

In agreement with the previous rolling experiments using VMRC-LCD cells expressing intact CD44, the beads coated with WT HABD exhibited rolling on the HA-coated surface. The beads coated with the PD-state mutant also firmly adhered to the HA surface, which was also consistent with the previous rolling experiments using mammalian cells. In addition, we designed the O-state mutant, in which the conformation is locked in the O state by an intradomain disulfide bond. Although the beads coated with the O-state mutant exhibited rolling under low-shear conditions, they were more easily detached at higher shear stress than those with WT HABD. These results unequivocally demonstrated that the two-state conformational equilibrium between the O and PD states is necessary for CD44-mediated rolling over a wide range of shear stresses.

Another important finding of this study is the effect of the mechanical force on the CD44-mediated rolling. Compared with the N-terminally attached HABD, the C-terminally attached HABD mediated more stable rolling at higher shear stress (Fig. 3 *B* and *C*). In contrast, no difference was observed for the beads coated with HABD mutants that adopt only the O state or the PD state (Fig. 3 *D–G*). These results strongly indicate that the tensile force applied from the C terminus of the HABD stabilizes the PD state. The mechanical regulation of CD44 is allosteric, as supported by SMD simulations (Fig. 4). The SMD simulations demonstrated that the pulling force disrupts the mechanically labile interaction between the α1 helix and the C-terminal mechanosensitive latch. In the O state, Tyr-161 forms hydrogen bonds with Glu-48 in the α1 helix of the Link module. At the same time, Glu-48 stabilizes the orientation of
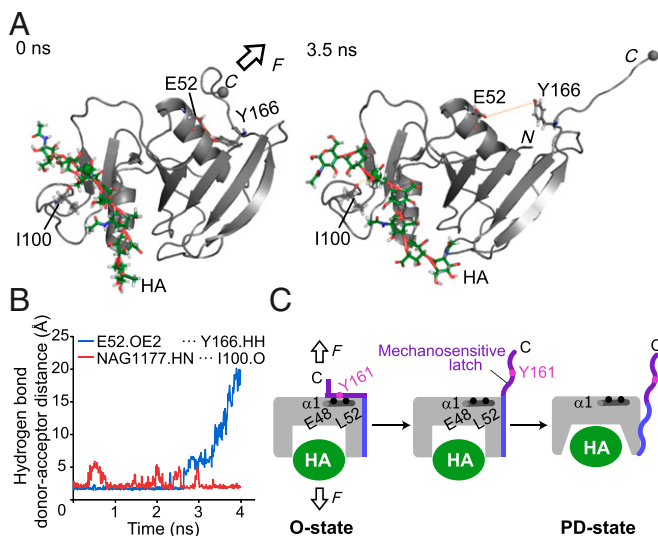
**Fig. 4.** Steered molecular dynamics (SMD) simulation of CD44 HABD by pulling force. (A) Snapshots of the HABD–HA8 complex at 0 ns (*Left*) and 3.5 ns (*Right*) during the SMD simulation. In the SMD simulation, the Cα carbon of the C-terminal residue Ile173 (gray sphere) was pulled at 10 Å/ns in the indicated direction (arrow), whereas the C2 atom of the *N*-acetylglucosamine residue (green sphere) was kept fixed. In the snapshot after 3.5 ns in the SMD simulation, the C-terminal mechanosensitive latch was completely separated from the α1 helix. (B) The time course of the hydrogen bond donor–acceptor distances between HA NAG1177 and I100 (red) and E52 and Y166 (blue). (C) Schematic depiction of the mechanosensitive latch in the force-induced conformational change of CD44 HABD.

the Lys-38 sidechain that forms a backbone hydrogen bond with Arg-41, which is critical for HA binding (Fig. S5) (24). Therefore, the disruption of the mechanosensitive latch interaction would disrupt this internal interaction network, thereby propagating the conformational change at the HA-binding site from the low- to the high-affinity state.

We postulated a mechanism of how the mechanical force stabilizes the HABD-mediated rolling under high shear stress. The HABD molecule at the leading edge of a rolling bead forms an initial contact with HA in the low-affinity O state (Fig. 5A). As the bead rolls on HA, the location of the HABD–HA bond reaches the rear end of the bead, resulting in the breakage of the bond at the rear end (Fig. 5B). Considering the diameter of the cell-sized bead (10 μm) and the tether length (12 nm), the maximum displacement of the beads (denoted as "contact zone," Fig. 5B) supported by a single HABD–HA bond is estimated to be 0.7 μm. The particle-tracking analyses demonstrated that the velocity of the beads moving on the HA substrate changes frame by frame (28) (Fig. S6A). As a result, more than half of the beads passed over the contact zone within ~80 ms, and about 80% passed within ~120 ms at a shear stress of 1.0 dyn/cm² (Fig. S6B). On the other hand, our previous NMR ZZ-exchange experiments revealed that the exchange rate between the O and PD states is on a timescale of 500 ms (21). Therefore, the duration of a single tether is too short for HABD to undergo the conformational transition from the O to the PD state, in the absence of force (Fig. 5D). However, when the tensile force is applied from the C terminus of HABD, the C-terminal mechanosensitive latch of HABD is immediately removed from the α1 helix, as shown by the SMD simulation, thereby inducing a further global conformational change to achieve the high-affinity PD state within 80 ms (Fig. 5D). As a result, the bonds at the rear end become more resistant to detachment and their lifetime will be prolonged, and the new bonds can be formed at the front side of the bead, before the bonds break at the rear end (Fig. 5C). In this manner, the rate of bond

dissociation at the rear end is balanced by the rate of new bond formation at the front edge, and the CD44-mediated rolling is stably sustained under high shear conditions. This model explains the impaired rolling ability of the mutant HABDs. Our present rolling experiments indicate that the rolling mediated by the O-state mutant was unstable, due to the weak shear resistance. This is because the O-state mutant loses the ability to undergo the conformational transition to the PD state, resulting in excess bond dissociation at the rear end relative to new bond formation at the leading edge (Fig. 5E). In contrast, the PD-state mutant exhibited only firm adhesion, rather than rolling. This behavior can be explained by the inability to undergo the conformational transition to the O state, resulting in excess new bond formation at the leading edge relative to the bond dissociation at the rear end (Fig. 5F).

As stated above, the estimated tether length between the HA on the surface and the HABD on the bead is 12 nm. The short tether length results in the steep bond angle of 88.7°, and the total force exerted on all HABD–HA bonds at a shear stress of 1.0 dyn/cm² is estimated to be 3.4 nN, which is 10 times larger than the force applied to the P-selectin–PSGL-1 bonds (28). Considering that an individual adhesion receptor–ligand noncovalent bond can bear forces in the range of 100 pN (10), the CD44-mediated rolling should be supported by a large number of bonds, compared with that mediated by selectin. It may be consistent with the fact that the HABD density on the beads in this study is 3,000–6,000 /μm², which is one order of magnitude higher than that in selectin-mediated rolling (27). In addition, it is expected that the unfolding of the C-terminal region will increase the tether length, which will reduce the total tensile force. Therefore, the tethers formed between the CD44–HA bonds are further stabilized upon the unfolding of the C-terminal segment, by a similar mechanism to that reported for type 1 pili of *Escherichia coli* (29).

In the previous study of the αL integrin I domain, it was hypothesized that the applied tensile force stabilizes the high-
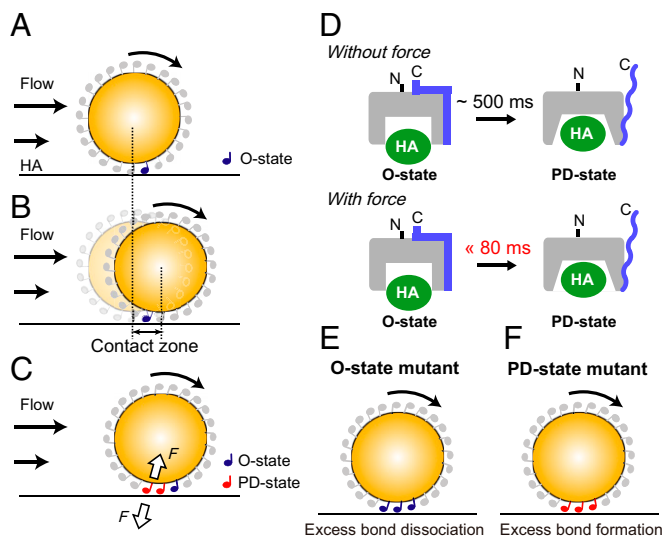


**Fig. 5.** Force-facilitated O-to-PD transition of CD44 HABD in rolling. (*A–C*) Schematic illustration of the effect of force on the HABD–HA interactions. (*A*) The initial contact with the HA ligand is mediated by HABD in the O state on the bead. (*B*) As the bead rolls, the location of the HABD–HA bond reaches the rear end of the bead. The maximum displacement of the bead mediated by a single HABD–HA bond is denoted as the "contact zone." (*C*) The tensile force exerted on the HABD–HA bond at the rear end induces the rapid conformational change to the PD state. (*D*) The O-to-PD transition rates, with or without tensile force. (*E* and *F*) Schematic diagram explaining the impaired rolling of the O-state mutant (*E*) and the PD-state mutant (*F*).

affinity state, by lowering the free energy of the high-affinity state relative to the low-affinity state (10). Here, we propose that the critical effect of the tensile force on the CD44–HA bond is to lower the energy barrier between the two states, rather than to lower the energy minimum of the PD state. Although the kinetic effect of mechanical force on receptor–ligand bonds was suggested in some systems (9, 30, 31), the significance of the increase in the transition rate for the adhesive function has not been reported so far, to our knowledge. Therefore, this is to our knowledge the first demonstration of the importance of the kinetic control of the tensile force in the adhesive function. It is possible that the force-induced rapid conformational transition may also regulate the adhesiveness mediated by other adhesion receptors, such as selectins and integrins (32).

CD44-mediated cell rolling is important in many physiological processes, such as leukocyte trafficking and hematopoietic progenitor cell homing to their niches. In addition, the involvement of rolling is also anticipated in pathological events, including the progression of atherosclerosis and cancer stem cell homing to specific niches (18, 33). In these processes, adhesive bonds are occasionally exposed to high levels of shear stress. For example, shear stress on bone marrow reaches ~8–30 dyn/cm$^2$, due to the mechanical loading and bending of bones (34). Our present findings provide the structural basis for the CD44-mediated cellular processes, which occur under high shear forces.

## Materials and Methods

The AviTag sequence was attached at either the C terminus or the N terminus of CD44 HABD (residues Q21–V178). The AviTagged HABDs were expressed and purified as described previously (22) and treated with biotin ligase BirA. The biotinylated HABD was attached to avidin-coated beads (Bangs Laboratory). The HABD mutants (Y161A and T47C/N164C) were generated using the QuikChange method (Stratagene).

In the cell-free rolling experiments, the HABD-coated beads were suspended at a density of $4 \times 10^4$/mL, in PBS containing 0.1% (wt/vol) BSA and 1 mM EDTA, and were perfused over the flow chamber, in which the bottom surface was coated with high-molecular-mass HA. In the detachment assays, the HABD-coated beads were perfused over the flow chamber at 0.3 dyn/cm$^2$ for 5 min and then subjected to increasing shear stress every 10 s up to 2.0 dyn/cm$^2$.

The SMD simulations were performed with the program NAMD2 (35). The crystal structure of the mouse CD44 HABD in complex with an HA 8mer [Protein Data Bank (PDB) code: 2JCR] (24) was used as the initial structure. During the simulations, the C2 atom of $N$-acetylglucosamine residue 1,177 was kept fixed, whereas the Cα atom of the mouse HABD C-terminal residue Ile-173 was pulled at a constant speed of 10 Å/ns with a spring constant of 1 kcal·mol$^{-1}$·Å$^{-2}$.

More detailed procedures are described in *SI Materials and Methods*.

1. Butcher EC, Picker LJ (1996) Lymphocyte homing and homeostasis. *Science* 272(5258): 60–66.
2. McEver RP, Zhu C (2010) Rolling cell adhesion. *Annu Rev Cell Dev Biol* 26:363–396.
3. Bell GI (1978) Models for the specific adhesion of cells to cells. *Science* 200(4342): 618–627.
4. Marshall BT, et al. (2003) Direct observation of catch bonds involving cell-adhesion molecules. *Nature* 423(6936):190–193.
5. Yakovenko O, et al. (2008) FimH forms catch bonds that are enhanced by mechanical force due to allosteric regulation. *J Biol Chem* 283(17):11596–11605.
6. Yago T, et al. (2008) Platelet glycoprotein Ibalpha forms catch bonds with human WT vWF but not with type 2B von Willebrand disease vWF. *J Clin Invest* 118(9):3195–3207.
7. Kong F, García AJ, Mould AP, Humphries MJ, Zhu C (2009) Demonstration of catch bonds between an integrin and its ligand. *J Cell Biol* 185(7):1275–1284.
8. Lee CY, et al. (2013) Actin depolymerization under force is governed by lysine 113: glutamic acid 195-mediated catch-slip bonds. *Proc Natl Acad Sci USA* 110(13): 5022–5027.
9. Thomas WE, Vogel V, Sokurenko E (2008) Biophysics of catch bonds. *Annu Rev Biophys* 37:399–416.
10. Astrof NS, Salas A, Shimaoka M, Chen J, Springer TA (2006) Importance of force linkage in mechanochemistry of adhesion receptors. *Biochemistry* 45(50):15020–15028.
11. Le Trong I, et al. (2010) Structural basis for mechanical force regulation of the adhesin FimH via finger trap-like beta sheet twisting. *Cell* 141(4):645–655.
12. Waldron TT, Springer TA (2009) Transmission of allostery through the lectin domain in selectin-mediated cell adhesion. *Proc Natl Acad Sci USA* 106(1):85–90.
13. Lou J, et al. (2006) Flow-enhanced adhesion regulated by a selectin interdomain hinge. *J Cell Biol* 174(7):1107–1117.
14. Aruffo A, Stamenkovic I, Melnick M, Underhill CB, Seed B (1990) CD44 is the principal cell surface receptor for hyaluronate. *Cell* 61(7):1303–1313.
15. DeGrendele HC, Estess P, Picker LJ, Siegelman MH (1996) CD44 and its ligand hyaluronate mediate rolling under physiologic flow: A novel lymphocyte-endothelial cell primary adhesion pathway. *J Exp Med* 183(3):1119–1130.
16. Bonder CS, Clark SR, Norman MU, Johnson P, Kubes P (2006) Use of CD44 by CD4+ Th1 and Th2 lymphocytes to roll and adhere. *Blood* 107(12):4798–4806.
17. Avigdor A, et al. (2004) CD44 and hyaluronic acid cooperate with SDF-1 in the trafficking of human CD34+ stem/progenitor cells to bone marrow. *Blood* 103(8): 2981–2989.
18. Cuff CA, et al. (2001) The adhesion receptor CD44 promotes atherosclerosis by mediating inflammatory cell recruitment and vascular cell activation. *J Clin Invest* 108(7): 1031–1040.
19. Teriete P, et al. (2004) Structure of the regulatory hyaluronan binding domain in the inflammatory leukocyte homing receptor CD44. *Mol Cell* 13(4):483–496.
20. Takeda M, et al. (2006) Ligand-induced structural changes of the CD44 hyaluronan-binding domain revealed by NMR. *J Biol Chem* 281(52):40089–40095.
21. Ogino S, et al. (2010) Two-state conformations in the hyaluronan-binding domain regulate CD44 adhesiveness under flow condition. *Structure* 18(5):649–656.
22. Takeda M, et al. (2003) Hyaluronan recognition mode of CD44 revealed by cross-saturation and chemical shift perturbation experiments. *J Biol Chem* 278(44):43550–43555.
23. Christophis C, et al. (2011) Shear stress regulates adhesion and rolling of CD44+ leukemic and hematopoietic progenitor cells on hyaluronan. *Biophys J* 101(3): 585–593.
24. Banerji S, et al. (2007) Structures of the Cd44-hyaluronan complex provide insight into a fundamental carbohydrate-protein interaction. *Nat Struct Mol Biol* 14(3):234–239.
25. Brunk DK, Goetz DJ, Hammer DA (1996) Sialyl Lewis(x)/E-selectin-mediated rolling in a cell-free system. *Biophys J* 71(5):2902–2907.
26. Sundd P, et al. (2012) 'Slings' enable neutrophil rolling at high shear. *Nature* 488(7411):399–403.
27. Yago T, et al. (2002) Distinct molecular and cellular contributions to stabilizing selectin-mediated rolling under flow. *J Cell Biol* 158(4):787–799.
28. Alon R, Chen S, Puri KD, Finger EB, Springer TA (1997) The kinetics of L-selectin tethers and the mechanics of selectin-mediated rolling. *J Cell Biol* 138(5):1169–1180.
29. Miller E, Garcia T, Hultgren S, Oberhauser AF (2006) The mechanical properties of E. coli type 1 pili measured by atomic force microscopy techniques. *Biophys J* 91(10): 3848–3856.
30. Kim J, Zhang CZ, Zhang X, Springer TA (2010) A mechanically stabilized receptor-ligand flex-bond important in the vasculature. *Nature* 466(7309):992–995.
31. Puklin-Faucher E, Gao M, Schulten K, Vogel V (2006) How the headpiece hinge angle is opened: New insights into the dynamics of integrin activation. *J Cell Biol* 175(2): 349–360.
32. Alon R, Dustin ML (2007) Force as a facilitator of integrin conformational changes during leukocyte arrest on blood vessels and antigen-presenting cells. *Immunity* 26(1): 17–27.
33. Zöller M (2011) CD44: Can a cancer-initiating cell profit from an abundantly expressed molecule? *Nat Rev Cancer* 11(4):254–267.
34. Weinbaum S, Cowin SC, Zeng Y (1994) A model for the excitation of osteocytes by mechanical loading-induced bone fluid shear stresses. *J Biomech* 27(3):339–360.
35. Phillips JC, et al. (2005) Scalable molecular dynamics with NAMD. *J Comput Chem* 26(16):1781–1802.